ЕКСПЕРИМЕНТАЛНО ИЗСЛЕДВАНЕ НА МИКРОСТРУКТУРАТА И СВОЙСТВАТА НА ПОВЪРХНОСТЕН СЛОЙ, ФОРМИРАН ЧРЕЗ ПЛАЗМЕНО НАПЛАСТЯВАНЕ

Христо Скулев, Технически университет, Варна
Георги Люцканов, ВВМУ "Н. Й. Вапцаров", Варна

EXPERIMENTAL STUDY OF THE MICROSTRUCTURE AND PROPERTIES OF SURFACE COATINGS FORMED BY PLASMA SPRAYING

Hristo Skulev, Technical University, Varna
Georgi Lyutskanov, Naval Academy „N. Y. Vaptsarov“, Varna

Abstract: *A study was performed to examine the characterization of the microstructure and properties of nickel plasma coatings obtained at different plasma conditions.*

The study was designed to assess the properties of Nickel Plasma Coatings based on the use of microscopic images, X-ray results, hardness measurements and Differential Scanning Calorimetry. The relationships between of the coating microstructures and properties were examined.

The phase composition of the nickel coatings is dependent on the plasma spraying regime apply during the formation of the plasma coatings. Different compositions of light and dark layers were present at different regimes. Amorphous state can be observed at room temperature but then changes to a homogenous structure when secondary heating was applied. The hardness of the coating increased after secondary heating up to 700°C but then decreased rapidly as it reached 1200°C. At different heating rates of 5-50°C/min only one exothermic peak can be seen on each sample. In addition, the increase of heating rate correspondingly increases the area of the DSC exothermic peaks. A relationship was established between the power (kW) of the spraying conditions with the ratio of the amorphous state in the coating. The results show that there are no effect on the ratio of amorphous state and the width of the peaks on the amorphous state (FWHM, °2Th) with the increase of power.

Key words: *Thermal spraying, Amorphous, Phase transitions, X-ray diffraction, Plasma spraying, Nickel alloy.*

1. INTRODUCTION

Thermal spraying is a generic term to describe a collection of coating processes involving material transport at high speeds and elevated temperature. Particles or droplets (of coating materials) are accelerated at high speeds, heated and are made to impact an object (i.e. the substrate). Successive particles thus reach a surface where the high energy causes the particles to deform and form a mechanical bond with the underlying surface. These particles vary depending upon the process, but can cover a range of 1 to 200 microns [1].

Plasma powder spraying method allows a large number of technological parameters to be varied. From previous research, it shows that a number of phase transformation occur takes place with the use of different parameters [2]. During secondary heating, the properties of the coating changes in microstructure and hardness. Therefore the aim of this project is to investigate the microstructure and properties of surface coating under different heating conditions.

New industrial applications and more demanding requirements of existing applications have pushed the thermal spray industry to produce even better coatings. This has become realized with greater control in the processing of materials with thermal spray. The processing conditions within each of the thermal spray technologies play a major role in the formation of the microstructure, phase composition and ultimately, the properties of the deposit. Continued efforts to further understand and improve upon the properties of the thermal spray deposit involve research in areas such as process and processing diagnostics, flame-particle interactions, splat formation, solidification dynamics and microstructure development [3].

This application is advanced new technology for surface treatment of materials. The idea of this technology is to use cheap materials as a based material and to apply plasma coatings with unique properties on the surface. As a result wear resistance, corrosion resistance, fatigue life, hardness the materials are significantly improved.

The project aims at characterization of the microstructure and properties of coatings obtained at different plasma conditions. The sample characterization includes hardness/microhardness measurements, X-ray analysis and microscopic study and the results from this experimental study will be very important for further extension of the application of this technology.

2. EXPERIMENTAL PROCEDURE

2.1. Composition of Plasma Powder and Regimes for Plasma Spraying

The chemical composition in atomic percent of the powder used for plasma spraying is given in Table 1. The coatings were sprayed on the 10mm diameter with 60mm length substrate, which were attached onto the rotating cylinder during plasma spraying process. The regimes for the plasma spraying are shown in Table 2.

Specimen with dimensions of 3.5mmx3.5mm were cut and used in the experimental study. The samples then mounted to hold and keep the specimens surface area flat during grinding and polishing. Thickness of the mount should be sufficient to enable of holding the mount firmly during grinding and polishing and thereby to prevent a rocking motion and to maintain a flat surface. After polishing, etching was done to optically enhance microstructural features such as grain size and phase features.

The sample the will be ready for to be experimented by using;

1) Differential Scanning Calorimetry (DSC) which measures the temperatures and heat flow associated with transitions in materials as a function of time and temperature.

2) Nikon Eclipse ME600 Metallurgical optical microscope used to get the microstructure images on a surface finish polished samples.

3) Mitutoyo HM-124 Hardness Machine to measure the hardness of the coating results.

4) X-Ray Diffraction to discover information about the structure of crystalline materials.

The integrated intensities of the phases (amorphous nickel) were calculated from the corresponding reflections in the XRD diffraction patterns of the deposit using the X'Pert Plus computer program.

3. RESULTS AND DISCUSSIONS

3.1. As Sprayed Coatings

3.1.1. Microstructure

From the studies of plasma spraying, it shows that the parameters of spraying regime have direct relationship with the microstructural characteristics of the coating. The regimes of the plasma coatings are shown in Table 2.

The cross-section analysis for microscopic images were prepared and subsequently polished.

The microstructure shows the variety of layering and stacking of coatings.

Table 1

Chemical composition in atomic percent of the powder

Element	Ni	Cr	C	Al	Si	Cu	W
%	73,1	12,8	5,1	2,0	6,5	0,3	0,2

Table 2

Regimes for Plasma Spraying

Sample	Base	Gas flow		Particle	Current	Voltage	Power
No	Material	l/min		Size	A	V	kW
	(Substrate)	Ar	N	µm			
1	Steel	20	2	60	350	52	18,2
2	Steel	30	6	60	350	70	24,5
3	Steel	20	2	60	550	51	28,1
4	Steel	30	6	60	550	70	38,5
5	Steel	25	4	60	550	61	33,6
6	Steel	30	6	60	450	69	31,1
7	Steel	25	4	60	450	60	27,0
N1	Steel	20	2	45	350	52	18,2
N2	Steel	30	6	45	350	70	24,5
N3	Steel	20	2	45	550	51	28,1
N4	Steel	30	6	45	550	70	38,5
N5	Steel	25	4	45	550	61	33,6
N6	Steel	30	6	45	450	69	31,1
N7	Steel	25	4	45	450	60	27,0
N8	Iron	20	2	45	350	52	18,2
N10	Iron	25	4	45	450	60	27,0
N11	Iron	30	6	45	550	70	38,5

As the power increased from 18.2kW to 38.5kW (Table 1), the deposition of layers increases as shown in Figure 1. The boundaries starts to disappear and the coatings approach homogenous layers with thickness of about 1-3im. The melted powder forming new elements is deposited in the form of layering with light and dark colours and the non-melted and partly melted particles have the round spherical shape (Figure 1 and 2). Sample 1 and 4 has more dark layers than light layers compare to sample N1 and N4. With the same regime for both samples, the only reason for this is that due to different powder particle size. Sample 1 and 4 has the larger powder particle (60 μm) than sample N1 and N4 (45 μm).

Plasma sprayed coatings with finer powders have finer and denser microstructures with less oxide inclusions. Coarse powders produce coarser and more open structured coatings with more oxidation than fine powders. This is mainly due to the differences in surface area of the powder particles exposed in the flame during spraying.

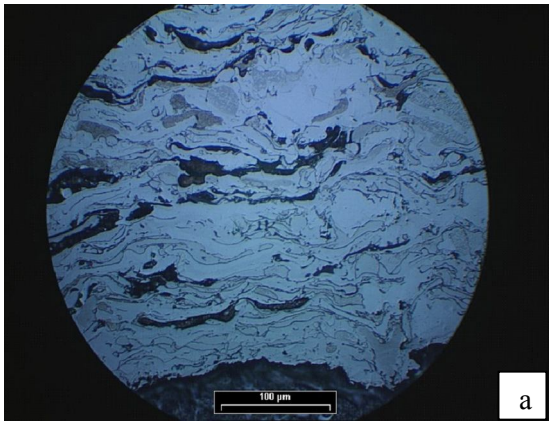

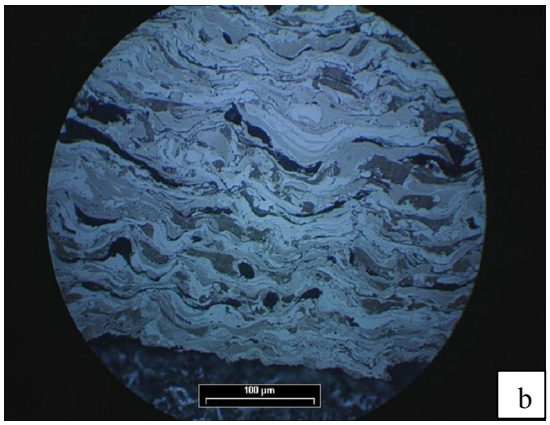

Figure 1. Microstructures of different sprayed conditions: a) Sample 1 at 18.2 kW; b) Sample 4 at 38.5 kW

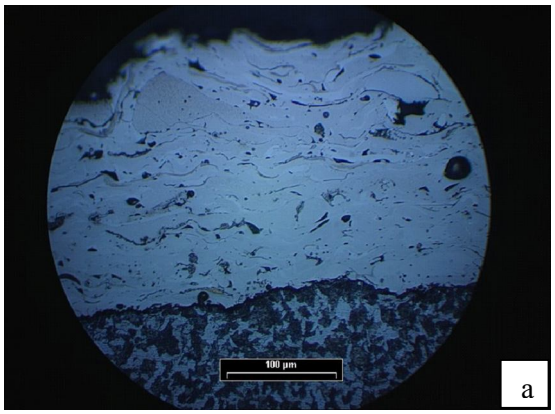

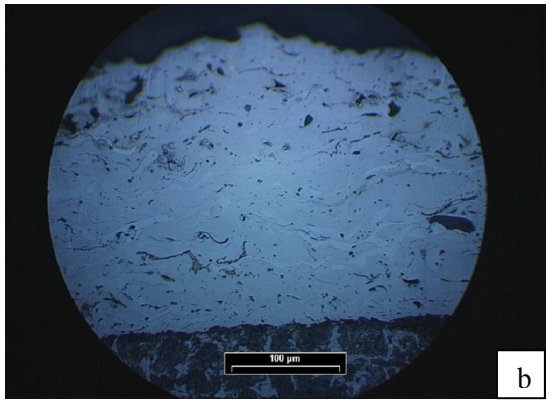

Figure 2. Microstructures of different sprayed conditions: a) Sample N1 at 18.2 kW; b) Sample N4 at 38.5 kW

The results from this analysis of the microstructure show that during all regimes spraying conditions, the bonding between the steel substrate and coating is very good, without any cracks and other defects.

3.1.2. Microhardness

Many factors such as chemical composition, spraying parameters and heat treatment have influence on the microhardness [4]. Microhardness across the cross-section of sample N5 and N7 was done for the measurements. Knoop indenter was used with load of 0.05 kg for 10 second.

Figure 3 illustrates the microhardness distribution of the coatings at room temperature. The tendency of the curve is not clear (Figure 3) and smoothing was done using the Mathlab programme to get the clear tendency of the curve (Figure 4).

A variation of hardness can be observed throughout the cross-sections ranging from 250 to 1284 HK0.05. Near the surface of the coating, the hardness value is low but then rises as the measurement reaches to the middle and decreases towards the substrate.

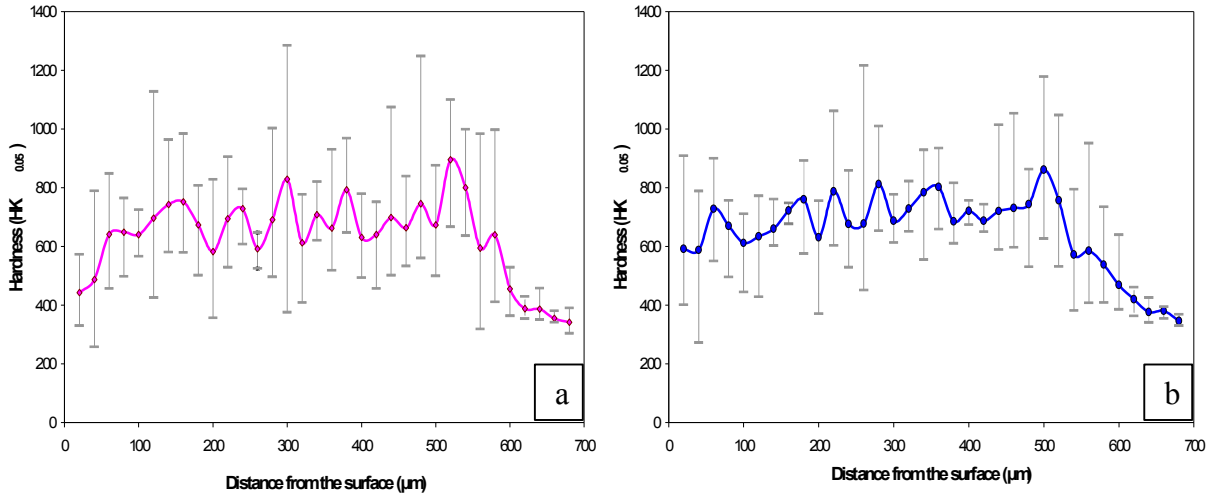

Figure 3. Microhardness profile for sprayed coating: a) Sample N5; b) Sample N7

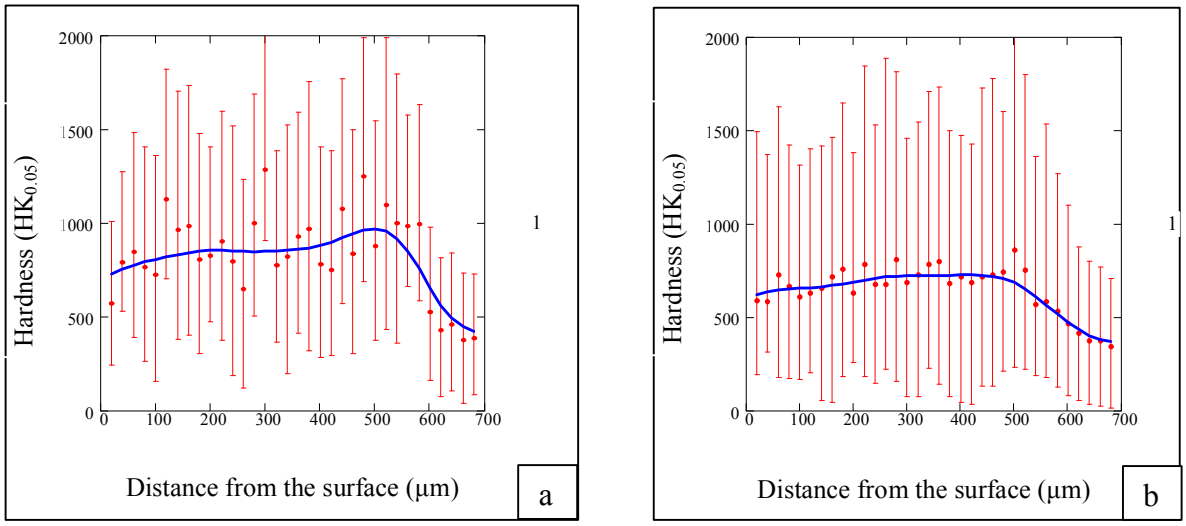

Figure 4. Microhardness profile for sprayed coating after smoothing: a) Sample N5; b) Sample N7

Observation was made during the measurement where the dark/black amorphous layers gave a low microhardness values in HK compared to the light layers. This illustrates that the variation of hardness is due to the different phases and chemical composition present at different position in the coating.

3.1.3. Differential Scanning Calorimetry

The effects of continuous heating process on the Nickel coating were investigated by using the DSC. The microstructural properties and phase transformation behaviour of the deposit were found to be associated with the effects of the heating rate and temperature.

Figure 5 shows the DSC curves of the sample at heating rates of 5-50°C/min. Only one exothermic peak can be seen in each of the DSC curves on each sample and the peak temperature for crystallisation to take place were determined. Based on the relationship in equation (1), a linear regression line could be obtained from the plot ln (Tm^2/φ) versus (1000/RTm).

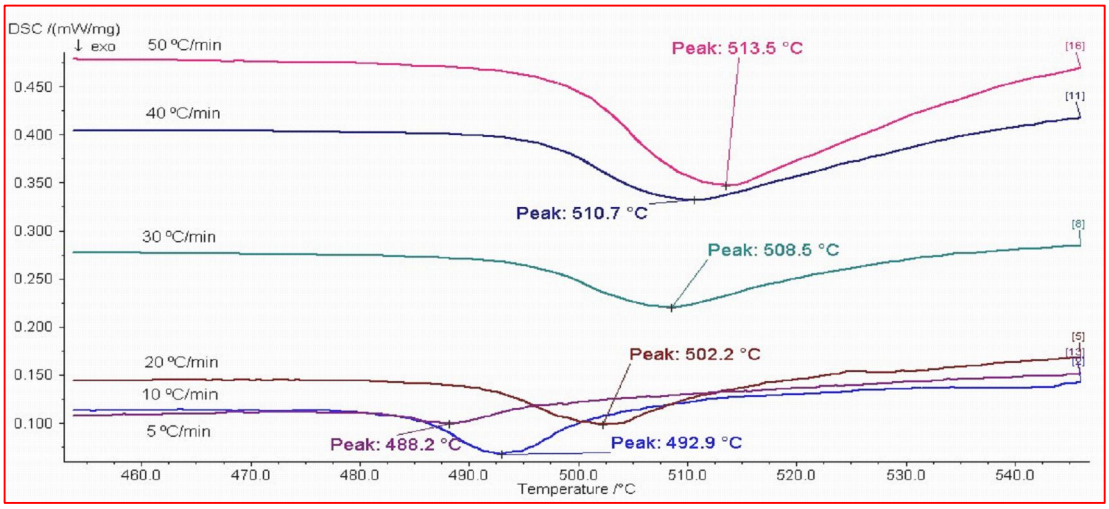

Figure 5. DSC curves of sample N7 at heating rates of 5-50°C/min

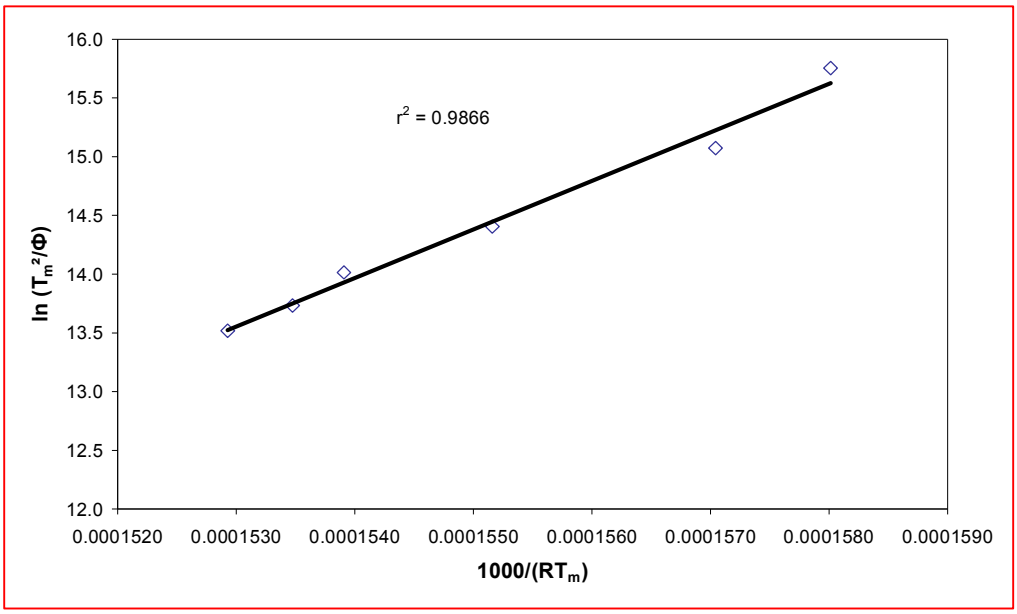

Figure 6. Slope of the plot ln (T_m^2/φ) versus ($1000/RT_m$) yielding the activation energy of sample N7 at maximum temperature of the DSC curves

The slope of this line yields the activation energy (Q) of the samples (Figure 6) [5].

(1) $$ln\left(\frac{T_m^2}{\varphi}\right) = \frac{Q}{RT_m} + ln\left(\frac{Q}{RK_0}\right) + ln(\beta) \quad ,$$

where φ is the heating rate in °C/sec, Tm is the maximum temperature (crystallisation temperature in °C, R is the gas constant 8.314 J/mol.K and Ko and β are constants.

The activation energy (Q) of the nickel coating calculated from the slope is 414.3kJ/mol.

In addition, the increase of heating rate correspondingly increases the area of the DSC exothermic peaks. It should be mention that the area of the DSC exothermic peak is equivalent to the total amount of heat flow during crystallisation process.

From the area of the exothermic peaks, a new relationship can be established by finding the degree of transformation of amorphous phase to crystal phase. This can be done by calculating the ratio of integrated intensity of the area (S1) to the total area of the exothermic peaks (S0) (Figure 7).

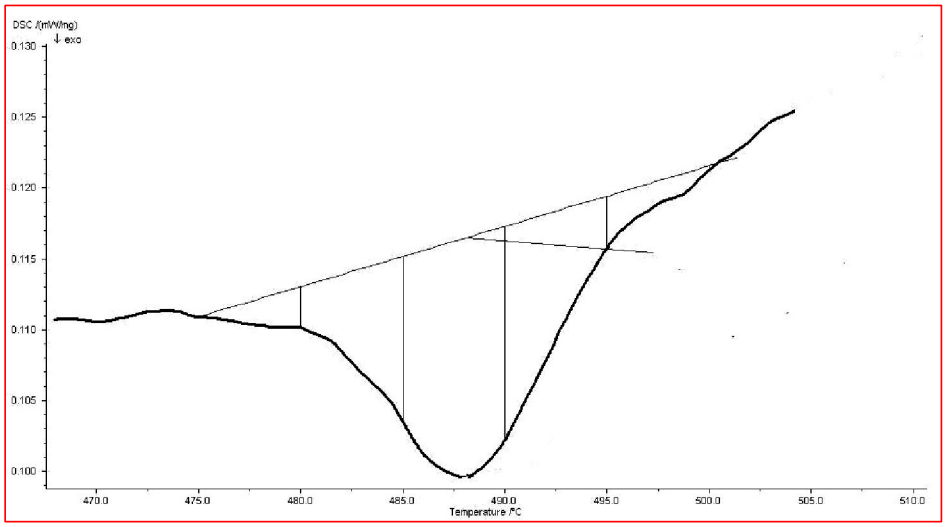

Figure 7. Graph of S_1 / S_0 (%) against temperature (°C)

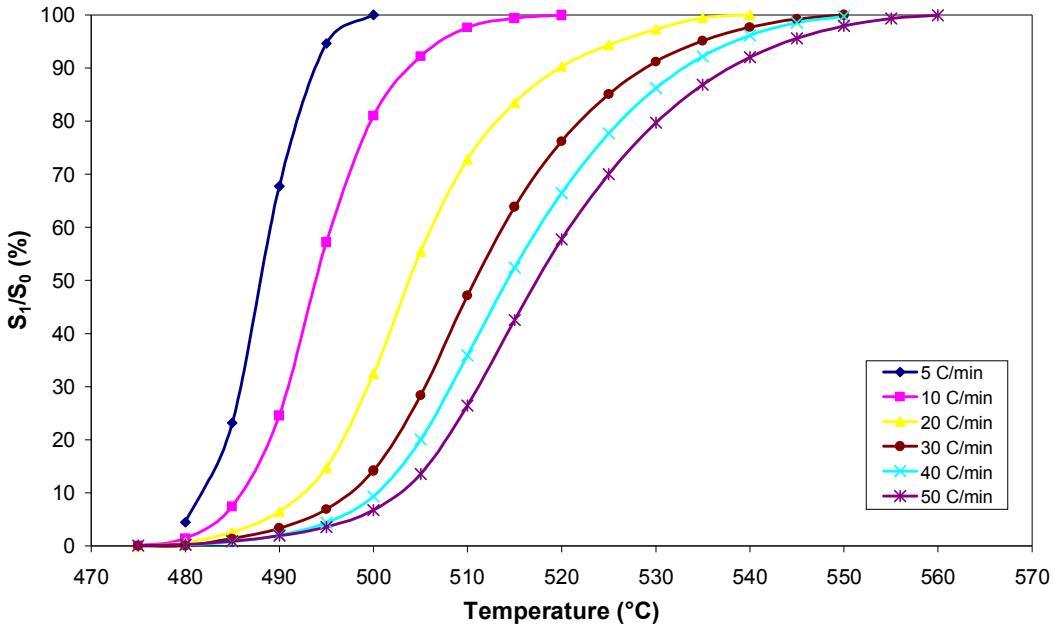

Figure 8. Variation of integrated intensity ratio (S_1 / S_0) over heating temperature

A graph of S1/S0 (%) against temperature (°C) was derived from this relationship (Figure 8). The graph shows that the temperature required forming a required percentage of amorphous and crystal in the coatings can be controlled. For example, to get the percentage of 50% amorphous and crystal present at a heating rate of 5°C/min, a heating temperature up to 489°C/min is needed. This will applies to all the heating rates up to 50°C/min.

Modification was done by using the temperature of each heating rates at 50% phase transformation (Figure 8) producing new graph (Figure 9). A better and more reliable result is established. The activation energy (Q) of the nickel coating after modification from the slope (Figure 9) is 362.3kJ/mol which is more accurate than 414.3kJ/mol.

3.1.4. X-ray Analysis

XRD were studied for sample N1-N7 to see whether the power used during the spraying process has any effect on the composition of the amorphous state in the coating. Figure 10 shows the XRD pattern of the as-coated nickel sample with a broad angular range amorphous profile, located at the 2θ position 40 - 50°. One high peak can be observed at the 2θ position located at 44 - 46°, four small peaks at 51- 53°, 76 - 78°, 91- 94° and 97- 98° approximately for all the samples. The presence of these broad-peak deflections and small-peaks indicates the coexistence of amorphous and crystalline nickel phases in the coating.

The crystalline phase is face centered cubic (fcc) structure. Apparently it is based on the fcc crystal

structure of the Ni that is the major element in the powder used for spraying [6-9].

A relationship was established between the power of the spray condition with the ratio of the amorphous state in the coating. It shows that there is no effect on the ratio of amorphous state with the increase of power (Figure 11). This also applies to the width of the peaks on the amorphous state (d-spacing, Å) where it shows no effect with the increase in power (Figure 12).

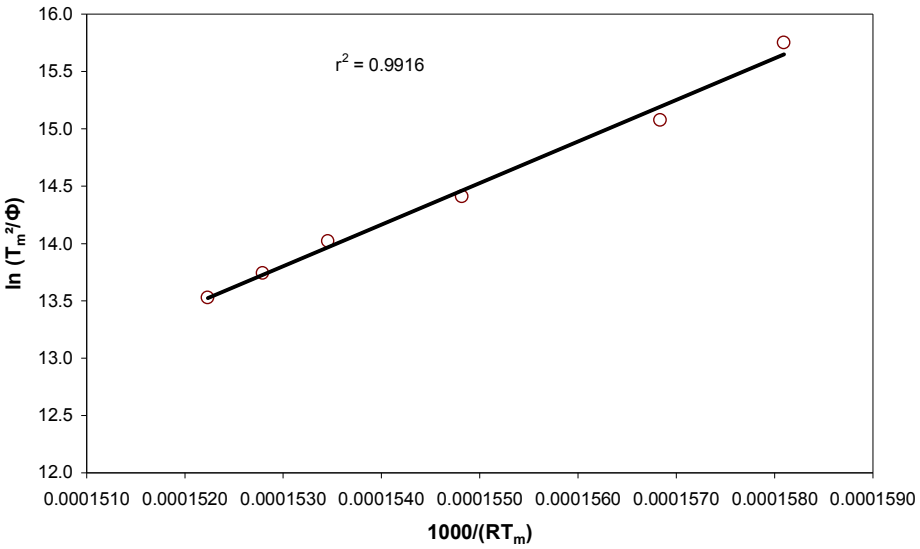

Figure 9. Modification of plot ln (T_m^2/φ) versus ($1000/RT_m$) yielding the activation energy of sample N7 at temperature of 50% of the phase transformation

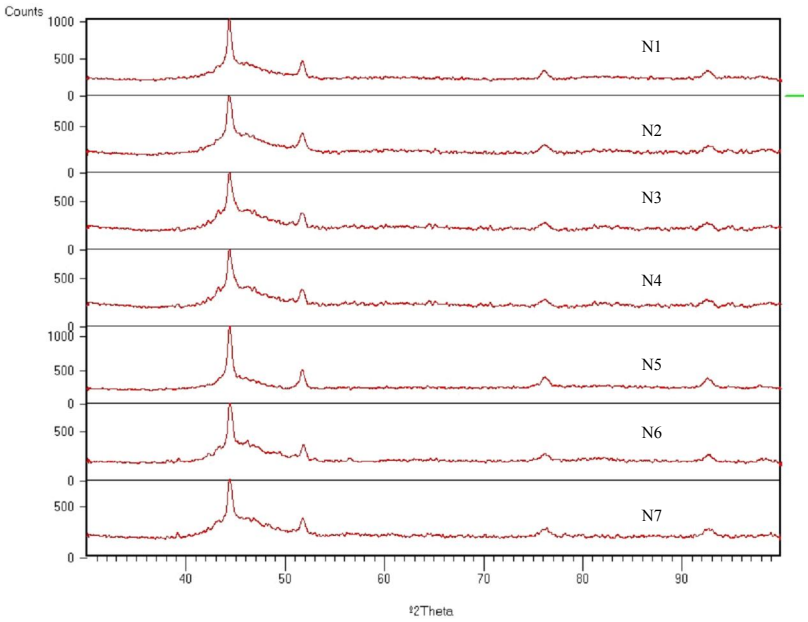

Figure 10. X-ray diffraction pattern for sample N1 ÷ N7 in as-coated conditions

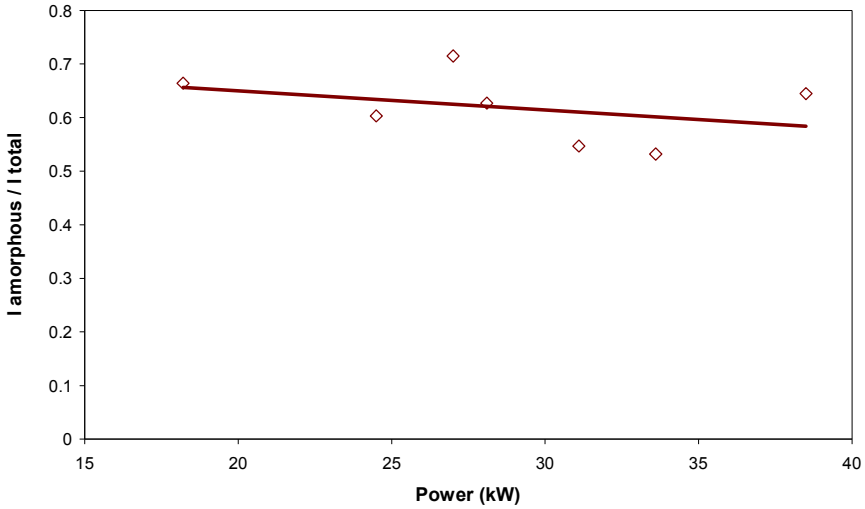

Figure 11. Relationship between ratio of amorphous state and power in as-coated conditions

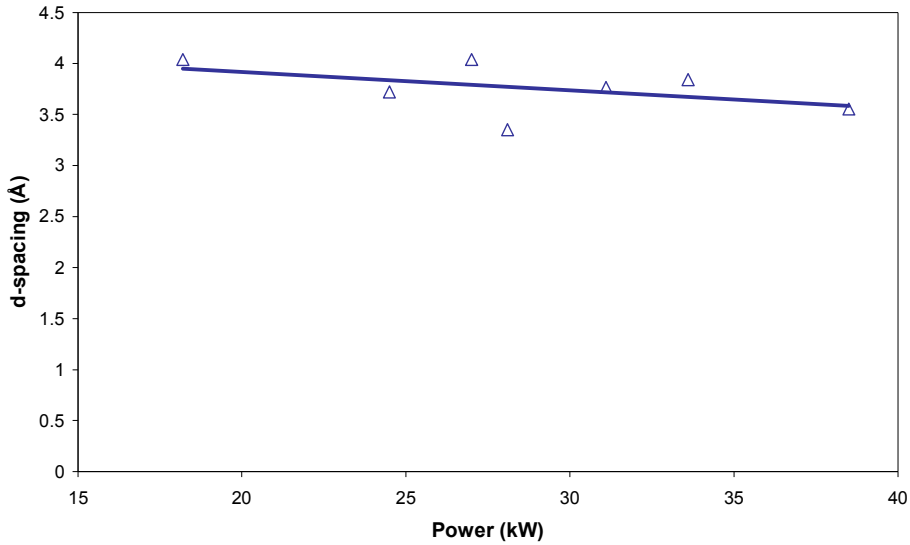

Figure 12. Relationship between d-spacing (Å) and power in as-coated conditions

3.2. After secondary heating

3.2.1. Microstructure

This study will be based on the formation of new phases when five samples from N7 were heated at a different temperature up to 565, 765, 965, 1035 and 1200°C.

Microstructure images were taken from the Nickel coatings at room temperature after the heating process. The samples were etched chemically before capturing the images.

The microstructures were studied and it shows that the microstructure of the coating does not change with the increase of temperature up to 700°C (Figure 13a, 13b, 13c). The images can be considered to have the lamellar microstructure although changes can be seen from lighter to dark layers at temperature up to 700°C. However, with the further increase of temperature to 1200°C led to the formation from lamellar to homogenous structures (Figure 13d, 13e, 13f). The layers start to disappear and the rounded spherical shapes of non-melted particles are dissolved. With further heating up to 1200°C, the initial compound present in the layers gained enough energy to form a new compound having a new homogenous light grains with no lamellar layers. Pores are not visible.

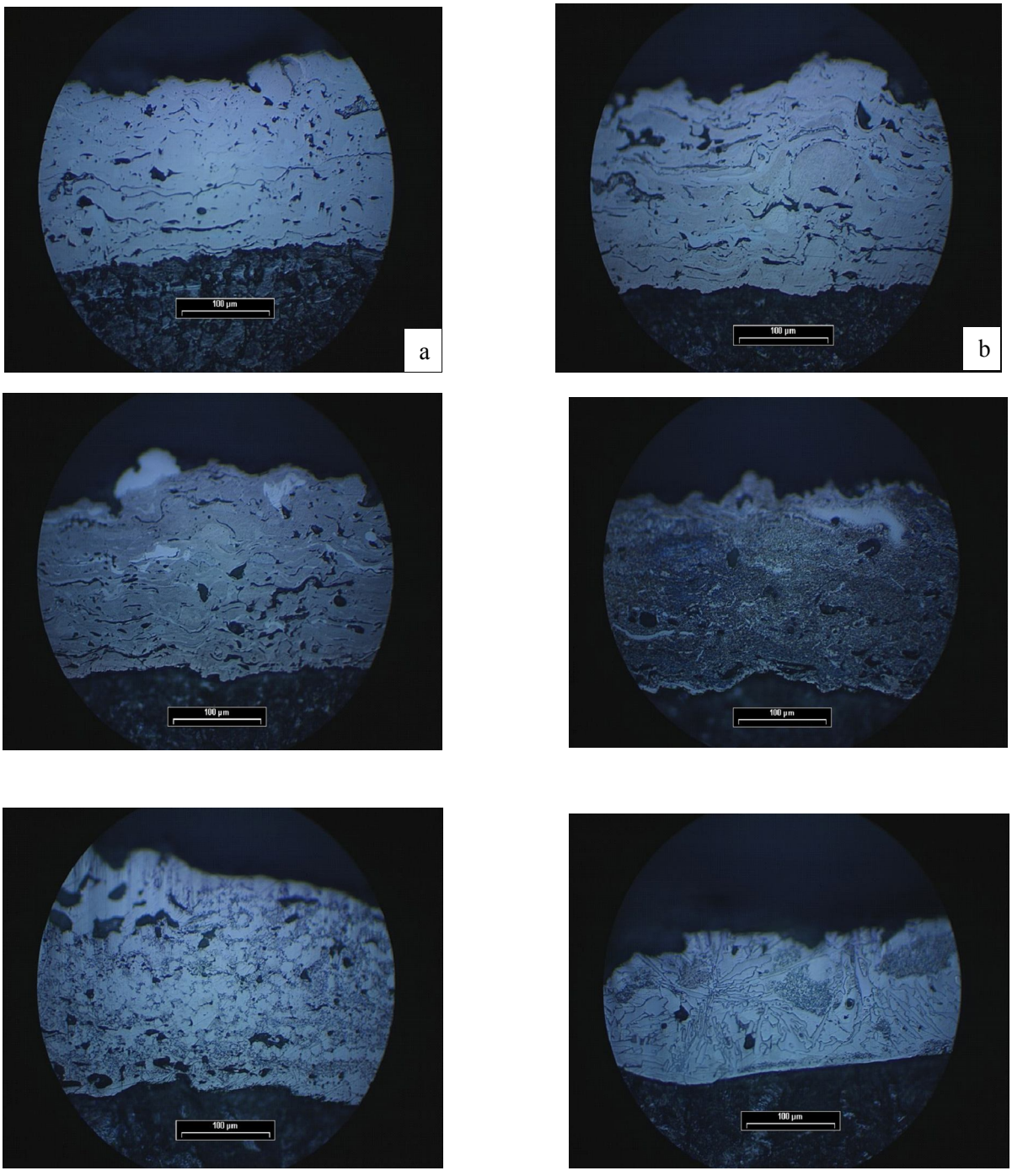

Figure 13. Microstructure of sample N7 after different heat treatments at magnification of x50: a) room temperature; b) 565°C; c) 700°C; d) 965°C; e) 1035°C; f) 1200°C

3.2.2. Microhardness

Vickers indenter was used with load of 1.0 kg for 5 seconds. The microhardness at the middle of the coatings was measured after the secondary heating. The heat treatment of sample N7 led to the improvement of the mechanical properties of the coating. A linear increase in microhardnes can be observed after heating was carried out to a temperature of 700°C. The microhardness then decreases after continuation of heat treatment to 1200°C (Figure 14). The measurement confirms that the homogenous structure formed after heat treatment from 700-1200°C has low microhardness (average 290 HV1.0) compare to the lamellar structure at room temperature (average 545 HV1.0) and lamellar structure heated to 700°C (685 HV1.0).

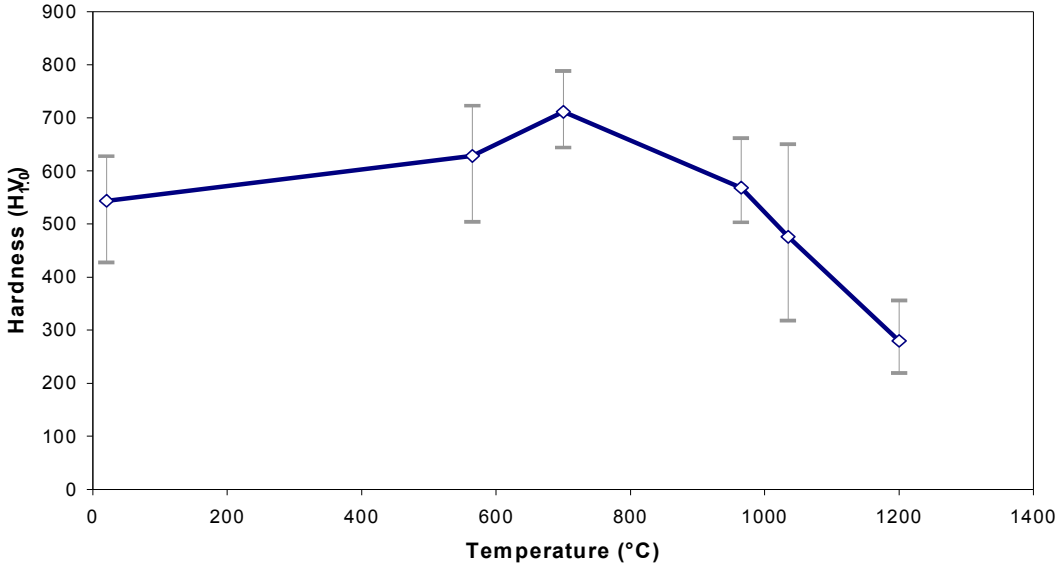

Figure 14. Microhardness of sample N7 after different heat

4. SUMMARY AND CONCLUSIONS

The microstructure shows the heterogeneous nature typical for the plasma where layering and stacking of the coating can be seen. With the increase of power, different microstructure was observed. The boundaries start to disappear and the coatings approach homogenous layers. After secondary heating from 700-1200°C, led to the formation from lamellar to homogenous structures where the layers start to disappear and the rounded spherical shapes of non-melted particles are dissolved.

The hardness as-sprayed is low near the coating, and then increases at the middle but decreases rapidly as it reached the substrate. After secondary heating, the hardness increases up to 700°C but then decreases on further heating to 1200°C. The change of the phase composition and microstructure after secondary heating led to the change of the hardness.

One exothermic peak were observed in each of the DSC curves at different heating rates of 5-50°C/min. From the relationship of equation (1), activation energy of the nickel is 414.3 kJ/mol when the maximum temperature of each heating rates value was used. However, a more accurate activation energy value of 363.2 kJ/mol was calculated when the temperature for 50% of the phase transformation on each heating rates was used.

One high peak and broad peak with 3 small peaks was observed for all samples N1-N7 after x-ray analysis. The broad-peak and small-peaks deflection indicates the coexistence of the amorphous and crystalline nickel phase in the coating. There are no relationship observed on the ratio of the amorphous and the width of the peaks of the amorphous state with the increase in power (kW).

REFERENCES

1. Н и к о в, Н. Влияние на електрода върху структурата на защитната струя. НК - 25 годишнина на ВМЕИ-Габрово, 1989, 125-127.

2. C h e n, W. L. T., E. Pfender, R. Spores, 'Power Metal Technologies and Application', ASM International, Materials Park, 1990, pp. 1065-1082.

3. D a v i s (ed.), J. R. Surface Hardening of Steels: Understanding the Basics, ASM International, Materials Park, OH, 2002.

4. K e o n g, KG; W. Sha, S. Malinov. 'Crystallisation kinetics and phase transformation behaviour of electroless nickel-phosphorus deposit with 6-9wt% phosphorus content' Acta Metallurgica Sinica (English Letters) (China), vol. 14, no. 6, pp. 419-424, Dec. 2001.

5. N i c o v, N., V. Gencheva. An Analytic model for gas atmosphere composition round the arc in underwater welding, Inter ocean technology 1990, Poland –Szechen, 249-254.

6. N i c o v, N., V. Gencheva. Simulation of gas of shelded zone in semi-automatic underwater welding, Inter ocean technology 1990, Poland –Szechen, 271-280.

7. K u l u, P., S. Zimakov. Surf Coat tech 130 (2000) 46.

8. S k u l e v, H., S. Malinov, W. Sha, P.A.M. Basheer. Microstructural and Mechanical Properties of Nickel-base Plasma Sprayed Coatings on Steel and Cast Iron Substrates, Surface & Coatings Technology, Vol. 197, n. 2-3, (2005), pp. 177-184.

9. S k u l e v, H., S. Malinov, P. A. M. Basheer, W. Sha. Modifications of Phases, Microstructure and Hardness of Ni-based Alloy Plasma Coatings due to Thermal Treatment, Surface & Coatings Technology, Vol. 185, n. 1, (2004), pp. 18-29.